AIRBORNE MIMO RADAR TRANSMIT-RECEIVE DESIGN UNDER SPECTRAL CONSTRAINT IN SIGNAL-DEPENDENT CLUTTER

Zhihui Li, Junpeng Shi, Dongming Wu, Shujie Shi, Qingsong Zhou

College of Electronic Engineering, National University of Defense Technology, Hefei, 230037, China

ABSTRACT

This paper considers the joint design of the transmit waveform and receive filter for airborne multiple-input multiple-output (MIMO) radar under spectral constraint in signal-dependent clutter. The spatial-frequency spectral compatibility constraint is imposed in the joint design problem. To tackle the non-convex joint design problem, we develop an iterative algorithm based on iterative feasible point pursuit successive convex approximation (FPP-SCA). The proposed algorithm can handle the non-convex terms by the convex approximation. Simulation results demonstrate the superiority of the proposed algorithm in terms of better signal-to-interference-plus-noise ratio (SINR) and better spectral compatibility ability.

Index Terms— airborne MIMO radar, joint design, spectral compatibility, FPP-SCA.

1. INTRODUCTION

In recent years, with the rapid development of wireless communication technology, the demand for spectrum bandwidth is increasing. How to realize the spectrum coexistence between radar and communication system has attracted more and more attention. Spectrum coexistence can be effectively realized through waveform design. Therefore, spectrum coexistence waveform design between radar and wireless communication system becomes a research hotspot [1]-[3].

To improve the target detection performance of airborne multiple-input multiple-output (MIMO) radar, the joint design of transmit waveform and receive filter for airborne MIMO radar has attracted considerable attention [4]-[9]. In [5], the authors studied the joint design problem of airborne MIMO radar and proposed five cyclic optimization algorithms for energy constraints, constant modulus constraints and similarity constraints to solve the joint design problem. Furthermore, they considered the constant modulus and finite-phase constraints of the waveform, and they proposed an efficient iterative algorithm by employing the dinkelbach transform and minimization maximization technology [6]. In [8], the authors first introduced the Riemannian geometric optimization method into the joint design problem of airborne MIMO radar. In the proposed algorithm, the constrained optimization problem is considered as an unconstrained optimization problem in the constrained search space, and the Riemannian gradient descent algorithm and the Riemannian trust region algorithm are proposed to solve the joint design problem. Some other references consider the joint design problem under the prior information of target uncertainties [10]-[13]. Note most existing studies on the joint design under the energy constraint, constant-modulus constraint, similarity constraint. However, the development of radio frequency systems such as radar, communication and electronic warfare makes the available spectrum resources more and more crowded [3], [14]. Thus, it is important to design spectral compatible waveforms for airborne MIMO radar to coexist with the communication system [15], [16].

In this letter, we develop an iterative algorithm to jointly design the transmit waveform and receive filter under the spectral constraint. The main contributions are summarized as follows: *1)* The spectral constraint is formed by considering the possible spatial angles and the possible frequency bands of the communication systems. *2)* We develop an iterative algorithm based on feasible point pursuit successive convex approximation (FPP-SCA) [17], which can transform the original non-convex problem into a convex one. The proposed algorithm can obtain a high quality solution through iteration. Simulation results validate that the proposed algorithm can achieve better output signal-to-interference-plus-noise ratio (SINR) and can form deep notches in the spatial-frequency regions of the communication systems.

Notation: We use boldface lowercase and uppercase letters to represent vectors and matrices, respectively. The superscripts $(\cdot)^*$, $(\cdot)^T$ and $(\cdot)^H$ represent the conjugate, transpose and conjugate transpose operators, respectively. $\mathbb{C}^{N\times N}$ denotes the $N \times N$ complex matrices. $\mathbf{I}_N$ denotes the $N \times N$ identity matrix and $\otimes$ is the Kronecker product. $\mathrm{vec}(\mathbf{A})$ stands for the vectorization of $\mathbf{A}$. $\mathrm{Re}(\cdot)$ and $|\cdot|$ mean, respectively, the real part and modulus of a complex number. $\|\cdot\|$ and $\|\cdot\|_\infty$ means the Euclidean and infinite norm, respectively. $\mathbb{E}(\cdot)$ denotes the expectation.

This work was supported in part by the National Natural Science Foundation of China under Grants 61901511, 62001510 and 62071476, in part by the Anhui Provincial Natural Science Foundation under Grant 2108085QF257, and in part by the Research Program of National University of Defense Technology under Grants ZK19-10, ZK20-22 and ZK20-33. (Corresponding author: Zhihui Li)

2. SIGNAL MODEL AND PROBLEM FORMULATION

Consider a collocated MIMO radar system equipped with a uniform linear arrays (ULA) of N_T transmit antennas and N_R receive antennas, where the inter-element spacing d equals half a wavelength. The height and velocity of the radar platform are v and H, respectively. The radar system transmits a burst of M pulses during the coherent processing interval (CPI) with the pulse repetition frequency (PRF) f_r. The transmit waveform is $\mathbf{S} \in \mathbb{C}^{N_T \times L}$, where L is the length of the code. The received signals are matched-filtered, down-converted and sampled. Then the received target, signal-dependent clutter and system noise signal can be expressed as [5]-[7]

$$\mathbf{y} = \alpha_t \mathbf{V}(f_t, \theta_t)\mathbf{s} + \sum_{p=-P}^{P} \sum_{k=1}^{N_c} \alpha_{c,p,k} \mathbf{V}(f_{c,p,k}, \theta_{c,p,k})\mathbf{s} + \mathbf{n}, \tag{1}$$

where $\mathbf{y} \in \mathbb{C}^{LMN_R \times 1}$, α_t, f_t and θ_t are the amplitude, normalized Doppler frequency and spatial angle of the target, respectively, $\alpha_{c,p,k}$, $f_{c,p,k}$ and $\theta_{c,p,k}$ are the amplitude, normalized Doppler frequency, and spatial angle of the kth clutter patch, respectively, $\mathbf{V}(f_t, \theta_t) = (\mathbf{u}(f_t) \otimes \mathbf{I}_L \otimes \mathbf{A}(\theta_t))$, where $\mathbf{A}(\theta_t) = \mathbf{b}(\theta_t)\mathbf{a}^T(\theta_t)$, with $\mathbf{u}(f_t) \in \mathbb{C}^{M \times 1}$, $\mathbf{a}(\theta_t) \in \mathbb{C}^{N_T \times 1}$ and $\mathbf{b}(\theta_t) \in \mathbb{C}^{N_R \times 1}$ being the temporal steering vector, transmit spatial and receive spatial steering vectors, respectively, $\mathbf{V}(f_{c,p,k}, \theta_{c,p,k}) = (\mathbf{u}(f_{c,p,k}) \otimes \mathbf{J}_P^T \otimes (\mathbf{A}(\theta_{c,p,k})))$ with $\mathbf{J}_p = \mathbf{J}_{-p}^T \in \mathbb{C}^{L \times L}$ being the shift matrix [5], $\mathbf{s} = \mathrm{vec}(\mathbf{S})$, $\mathbf{n} \in \mathbb{C}^{LMN_R \times 1}$ stands for the complex white Gaussian noise with zero mean and covariance matrix $\sigma_n^2 \mathbf{I}_{LMN_R}$, where σ_n^2 is the noise power. For simplicity, $\mathbf{V}(f_{c,p,k}, \theta_{c,p,k})$ is denoted by $\mathbf{V}_{c,p,k}$ in the following.

To improve target detection performance in the signal-dependent clutter, the output SINR of receive filter is maximized. Thus, the received signals are filtered by the receive filter $\mathbf{w} \in \mathbb{C}^{LMN_R \times 1}$, and the output SINR can be given by

$$\mathrm{SINR}(\mathbf{s}, \mathbf{w}) = \frac{\sigma_t^2 |\mathbf{w}^H \mathbf{V}(f_t, \theta_t)\mathbf{s}|^2}{\mathbf{w}^H \mathbf{\Phi}_{\mathrm{cn}}(\mathbf{s})\mathbf{w}}, \tag{2}$$

where

$$\mathbf{\Phi}_{\mathrm{cn}}(\mathbf{s}) = \sum_{p=-P}^{P} \sum_{k=1}^{N_c} \sigma_{c,p,k}^2 \mathbf{V}_{c,p,k} \mathbf{s}\mathbf{s}^H \mathbf{V}_{c,p,k}^H + \sigma_n^2 \mathbf{I}_{LMN_R},$$

with $\sigma_t^2 = \mathbb{E}\{|\alpha_t|^2\}$ and $\sigma_{c,p,k}^2 = \mathbb{E}\{|\alpha_{c,p,k}|^2\}$.

In this paper, we consider the constaint modulus constraint, similarity constraint, and the spectral constraint on the transmit waveform $\mathbf{s}$. Specifically, the constraint modulus constraint $|\mathbf{s}(i)| = 1/\sqrt{N_T L}, \forall i$ is imposed to avoid excessive amplitude modulation. The similarity constraint is imposed to obtain the desired features of the transmit waveform, i.e., $\|\mathbf{s} - \mathbf{s}_r\|_\infty \leq \xi$, where the parameter ξ rules the similarity between $\mathbf{s}$ and reference waveform $\mathbf{s}_r$. Furthermore, the spectral constraint is considered to guarantee the spectral compatibility with overlaid communication systems. Concretely, assume that each communication system occupy a frequency band $\Psi = [f_l^r, f_u^r], r = 1, \cdots, R$, where f_l^r and f_u^r represent the lower and upper normalized frequencies of the rth system. In addition, consider that the each communication system locates in a normalized spatial angle $\Theta = [\sin(\theta_l^r), \sin(\theta_u^r)]$, where θ_l^r and θ_u^r stand for the lower and upper spatial angles, respectively. Thus, the spectral constraint can be defined as [1], [15], [16], [18]

$$\mathbf{s}^H \mathbf{\Phi} \mathbf{s} \leq \zeta, \tag{3}$$

where ζ represent the permissible total transmit waveform energy in all spatial-frequency bands, and $\mathbf{\Phi}$ is calculated by [1]

$$\mathbf{\Phi} = \sum_{r=1}^{R} \gamma_r (\mathbf{F}^r \otimes \mathbf{U}^r), \tag{4}$$

where γ_r represents the coefficient to control the waveform energy in the rth spatial-frequency band, $\mathbf{F}^r \in \mathbb{C}^{L \times L}$ and $\mathbf{U}^r \in \mathbb{C}^{N_T \times N_T}$ can be computed by

$$\mathbf{F}^r(p_1, p_2) = \begin{cases} f_u^r - f_l^r, & p_1 = p_2 \\ \frac{e^{j2\pi f_u^r (p_1 - p_2)} - e^{j2\pi f_l^r (p_1 - p_2)}}{j2\pi(p_1 - p_2)}, & p_1 \neq p_2, \end{cases} \tag{5}$$

and

$$\mathbf{U}^r(q_1, q_2) = \begin{cases} (v_u^r - v_l^r)/N_T, & q_1 = q_2 \\ \frac{1}{N_T} \frac{e^{j\pi v_u^r (q_1 - q_2)} - e^{j\pi v_l^r (q_1 - q_2)}}{j\pi(q_1 - q_2)}, & q_1 \neq q_2, \end{cases} \tag{6}$$

where $v_u = \sin(\theta_u)$ and $v_l = \sin(\theta_l)$.

Therefore, leveraging on the aforementioned discussions, the joint design of transmit waveform and receive filter can be formulated as the following constrained optimization problem

$$\mathcal{P} \begin{cases} \max\limits_{\mathbf{s}, \mathbf{w}} \ \mathrm{SINR}(\mathbf{s}, \mathbf{w}) \\ |\mathbf{s}(i)| = 1/\sqrt{N_T L}, \forall i, \\ \mathbf{s}^H \mathbf{\Phi} \mathbf{s} \leq \zeta, \\ \|\mathbf{s} - \mathbf{s}_r\|_\infty \leq \xi. \end{cases} \tag{7}$$

Problem $\mathcal{P}$ is NP-hard because of the non-convex objective function and non-convex constraints. In the following, we present an iterative algorithm based on FPP-SCA to deal with $\mathcal{P}$.

3. TRANSMIT-RECEIVE DESIGN FOR $\mathcal{P}$

In this section, we focus on the joint design of transmit waveform and receive filter. We develop an iterative algorithm to obtain a high quality solution to problem $\mathcal{P}$. Specifically, the receive filter $\mathbf{w}$ is optimized for a fixed $\mathbf{s}$. Then the transmit waveform $\mathbf{s}$ is optimized for a fixed $\mathbf{w}$.

3.1. Receive Filter Optimization

The optimization problem (7) with respect to $\mathbf{w}$ with a given $\mathbf{s}$ is equivalent to

$$\max_{\mathbf{w}} \ \frac{|\mathbf{w}^H\mathbf{V}(f_t,\theta_t)\mathbf{s}|^2}{\mathbf{w}^H\mathbf{\Phi}_{\rm cn}(\mathbf{s})\mathbf{w}} \tag{8}$$

Problem (8) is can be equivalently transformed into the well-known minimum variance distortionless response (MVDR) problem, whose solution can be given by

$$\mathbf{w} = \frac{\mathbf{\Phi}_{\rm cn}^{-1}(\mathbf{s})\mathbf{V}(f_t,\theta_t)\mathbf{s}}{\mathbf{s}^H\mathbf{V}^H(f_t,\theta_t)\mathbf{\Phi}_{\rm cn}^{-1}(\mathbf{s})\mathbf{V}(f_t,\theta_t)\mathbf{s}}. \tag{9}$$

3.2. Transmit Waveform Optimization

Substituting (9) into (7), and after some algebraic manipulations, the problem (7) is transformed as

$$\mathcal{P}\begin{cases} \max\limits_{\mathbf{s},\mathbf{w}} \ \mathbf{s}^H\mathbf{Q}(\mathbf{s})\mathbf{s} \\ |\mathbf{s}(i)| = 1/\sqrt{N_TL}, \forall i, \\ \mathbf{s}^H\mathbf{\Phi}\mathbf{s} \le \zeta, \\ \|\mathbf{s}-\mathbf{s}_r\|_\infty \le \xi. \end{cases} \tag{10}$$

where $\mathbf{Q}(\mathbf{s}) = \mathbf{V}^H(f_t,\theta_t)\mathbf{\Phi}_{\rm cn}^{-1}(\mathbf{s})\mathbf{V}(f_t,\theta_t)$. Problem (10) is a non-convex optimization problem. To tackle this problem, we transform the maximization problem (10) into a minimization problem

$$\begin{cases} \min\limits_{\mathbf{s}} -\mathbf{s}^H\mathbf{Q}(\mathbf{s})\mathbf{s} \\ (1) \ |\mathbf{s}(i)| = 1/\sqrt{N_TL}, \forall i, \\ (2) \ \mathbf{s}^H\mathbf{\Phi}\mathbf{s} \le \zeta, \\ (3) \ \|\mathbf{s}-\mathbf{s}_r\|_\infty \le \xi. \end{cases} \tag{11}$$

However, the problem (11) is still non-convex due to the non-convexity of the objective function, the first constraint and the second constraint. In the following, we employ the SCA framework to cope with the non-convex constraints.

Since $\mathbf{Q}(\mathbf{s})$ is a positive semidefinite matrix. According to the SCA approach [17], we can obtain a lower bound of $\mathbf{s}^H\mathbf{Q}(\mathbf{s})\mathbf{s}$ for any arbitrary feasible point $\mathbf{s}_0$. Specifically, we have $(\mathbf{s}-\mathbf{s}_0)^H\mathbf{Q}(\mathbf{s})(\mathbf{s}-\mathbf{s}_0) \ge 0$ for any $\mathbf{s}_0$. Expanding the left-hand side of the inequality, we have

$$\mathbf{s}^H\mathbf{Q}(\mathbf{s})\mathbf{s} \ge 2{\rm Re}(\mathbf{s}^H\mathbf{Q}(\mathbf{s})\mathbf{s}_0) - \mathbf{s}_0^H\mathbf{Q}(\mathbf{s})\mathbf{s}_0. \tag{12}$$

According to (12), we may utilize the linear approximation around $\mathbf{s}_0$ to replace the non-convex objective function, i.e.,

$$-\mathbf{s}^H\mathbf{Q}(\mathbf{s})\mathbf{s} \le \mathbf{s}_0^H\mathbf{Q}(\mathbf{s})\mathbf{s}_0 - 2{\rm Re}(\mathbf{s}^H\mathbf{Q}(\mathbf{s})\mathbf{s}_0). \tag{13}$$

The first constraint can be rewritten as $|\mathbf{s}(i)|^2 - 1/N_TL \le 0$ and $|\mathbf{s}(i)|^2 - 1/N_TL \ge 0$, respectively. The former is a convex constraint while the latter is non-convex. Then we employ the first-order condition [19] for the convex function to achieve the lower bound of $|\mathbf{s}(i)|^2$, that is

$$\begin{aligned} |\mathbf{s}(i)|^2 &\ge |\mathbf{s}_0(i)|^2 + {\rm Re}\{(\frac{\partial|\mathbf{s}(i)|^2}{\partial\mathbf{s}(i)})^*(\mathbf{s}(i)-\mathbf{s}_0(i))\} \\ &= |\mathbf{s}_0(i)|^2 + {\rm Re}\{2\mathbf{s}_0^*(i)(\mathbf{s}(i)-\mathbf{s}_0(i))\}. \end{aligned} \tag{14}$$

Substituting (14) into $|\mathbf{s}(i)|^2 - 1/N_TL \ge 0$, we have

$$\begin{aligned} 1/N_TL - |\mathbf{s}(i)|^2 \le 1/N_TL - |\mathbf{s}_0(i)|^2 - \\ {\rm Re}\{2\mathbf{s}_0^*(i)(\mathbf{s}(i)-\mathbf{s}_0(i))\} \le 0. \end{aligned} \tag{15}$$

After some manipulations, we obtain

$$1/N_TL - 2{\rm Re}\{\mathbf{s}_0^*(i)\mathbf{s}(i)\} + |\mathbf{s}_0(i)|^2 \le 0, \forall i. \tag{16}$$

The last constraint of problem (11) can be expressed as

$$|\mathbf{s}(i)-\mathbf{s}_r(i)|^2 \le \xi^2, \forall i. \tag{17}$$

Finally, substituting all non-convex constraints in (11) with their convex approximations in (13), (16) and (17), we have

$$\begin{cases} \min\limits_{\mathbf{s}} \ \mathbf{s}_0^H\mathbf{Q}(\mathbf{s})\mathbf{s}_0 - 2{\rm Re}(\mathbf{s}^H\mathbf{Q}(\mathbf{s})\mathbf{s}_0) \\ |\mathbf{s}(i)|^2 - 1/N_TL \le 0, \\ 1/N_TL - 2{\rm Re}\{\mathbf{s}_0^*(i)\mathbf{s}(i)\} + |\mathbf{s}_0(i)|^2 \le 0, \forall i, \\ \mathbf{s}^H\mathbf{\Phi}\mathbf{s} \le \zeta, \\ |\mathbf{s}(i)-\mathbf{s}_r(i)|^2 \le \xi^2, \forall i. \end{cases} \tag{18}$$

It is worth noting that the problem (18) may have one feasible solution $\mathbf{s}_0$ because the constraints $|\mathbf{s}(i)|^2 - 1/N_TL \le 0$ and $1/N_TL - 2{\rm Re}\{\mathbf{s}_0^*(i)\mathbf{s}(i)\} + |\mathbf{s}_0(i)|^2 \le 0$ have only one intersection $(t_0,\mathbf{s}_0)$. Inspired by the idea of FPP procedure [17], [18], we introduce a set of slack variables $\mathbf{u}$ to the second constraint in problem (18) and add the norm term $\|\mathbf{u}\|$ in the objective function. Then the problem (18) is cast as

$$\begin{cases} \min\limits_{\mathbf{s}} \ \mathbf{s}_0^H\mathbf{Q}(\mathbf{s})\mathbf{s}_0 - 2{\rm Re}(\mathbf{s}^H\mathbf{Q}(\mathbf{s})\mathbf{s}_0) + \varrho\|\mathbf{u}\| + \\ \qquad\qquad \kappa\|\mathbf{s}-\mathbf{s}^{(n-1)}\|^2 \\ |\mathbf{s}(i)|^2 - 1/N_TL \le 0, \\ 1/N_TL - 2{\rm Re}\{(\mathbf{s}^{(n-1)})^*(i)\mathbf{s}(i)\} + |\mathbf{s}^{(n-1)}(i)|^2 \\ \qquad\qquad -\mathbf{u}(i) \le 0, \forall i, \\ \mathbf{s}^H\mathbf{\Phi}\mathbf{s} \le \zeta, \\ |\mathbf{s}(i)-\mathbf{s}_r(i)|^2 \le \xi^2, \forall i, \\ \mathbf{u}(i) \ge 0, \forall i, \end{cases} \tag{19}$$

where ϱ and κ are positive parameters, $(\mathbf{s}^{(n-1)}, t^{(n-1)})$ is the $(n-1)$th iteration solution for the problem (19) and the initial iteration solution is $(\mathbf{s}^{(0)}, t^{(0)})$. The term $\|\mathbf{s}-\mathbf{s}^{(n-1)}\|^2$ in problem (19) is employed to ensure that the solutions between adjacent iterations are same. It is seen that the problem (19) is a convex QCQP problem, and it can be converted into a second-order cone programming (SOCP) problem. Then the problem (19) can be resolved by CVX toolbox [20] with a polynomial time computational complexity of $\mathcal{O}((N_TL)^{3.5})$. Finally, the main procedures of the joint design of $\{\mathbf{w}_{n_1,n_2},\mathbf{s}\}$ are achieved.

4. SIMULATIONS

In this section, we compare the performance of the proposed joint design method with the state-of-the-art methods in the literature. All the simulations are performed on the Matlab 2016b under a PC with an Intel i7-9750U CPU and 32 GB RAM. For airborne MIMO radar system settings, the numbers of the transmit antenna and the receive antenna are $N_T = 6$ and $N_R = 6$, respectively. The system transmits $M = 6$ pulses during a CPI with the PRF being $f_r = 2000$. The code length is $L = 10$. The platform height is 9000 m and the velocity is 150 m/s. The actual position of the target is configured as $(0.2, -0.2)$, and the power of which is 20 dB. For the clutter, we set $P = 1$, $N_c = 181$, $\sigma_{c,p,k} = 1$, $p = -P, \cdots, P$, $k = 1, \cdots, N_c$. Consider two communication systems with the frequency bands being $\Psi_1 = [0.6, 0.7]$ and $\Psi_2 = [0.3, 0.4]$, respectively. The normalized spatial angles are $\Theta_1 = [-0.6, -0.5]$ and $\Theta_2 = [0.6, 0.7]$. The coefficients in (4) are set to be $\gamma_1 = \gamma_2 = 1$. The noise power is 0 dB. The orthogonal linear frequency modulation (LFM) is chosen as the reference waveform vector $\mathbf{s}_r$ [18], [21]. For the proposed algorithm, we set $\varrho = 50$, $\kappa = 10^{-5}$. The simulations of SDP and randomization (SDP-R) algorithm [21] are also provided for comparison, and the number of randomization trials is 500. The total waveform energy constraint in the two communication systems is $\zeta = 0.00005$, and the termination value for all these algorithms is set to be $\epsilon = 10^{-4}$.

Fig. 1 presents the output SINR versus the number of iterations of the SDP-R algorithm and the proposed algorithm with $\xi_0 = 0.4, 1, 1.6$ ($\xi_0 = \xi\sqrt{N_T L}$). It is seen that the SINR values of all algorithms increase with ξ_0. Apparently, the proposed algorithm performs better than SDP-R algorithm with different ξ_0.

Fig. 2 plots the spatial-frequency power spectra of designed waveforms by different algorithms. The black rectangles represent the spatial-frequency region of the two communication systems. It is seen from Fig. 2 (a), (b) and (c) that the SDP-R algorithm cannot form deep notches in the spatial-frequency region of two communication systems. Contrarily, it is clearly observed that the proposed algorithm forms deep notches in the spatial-frequency power spectra for all ξ_0. This validates the spectrum compatible of the proposed algorithm.

5. CONCLUSION

This paper studies the joint design problem of the transmit waveform and receive filter for airborne MIMO radar under spectral constraint. To tackle the non-convex joint design problem, we develop an iterative algorithm based on FPP-SCA. Simulation results show that that the proposed algorithm achieves higher output SINR, and more deep notches in the spatial-frequency region of the communication systems. Future research interests may include joint design problem under the inaccurate information about the communication systems [22].

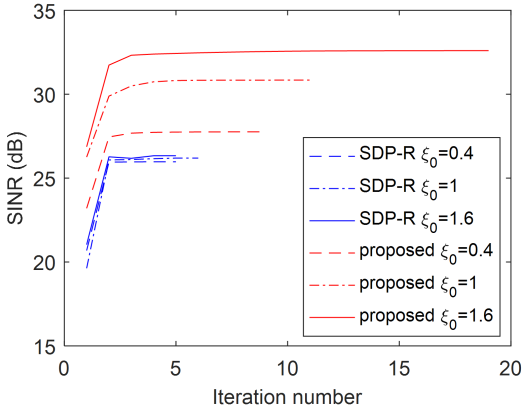

Fig. 1: SINR versus the iteration number.

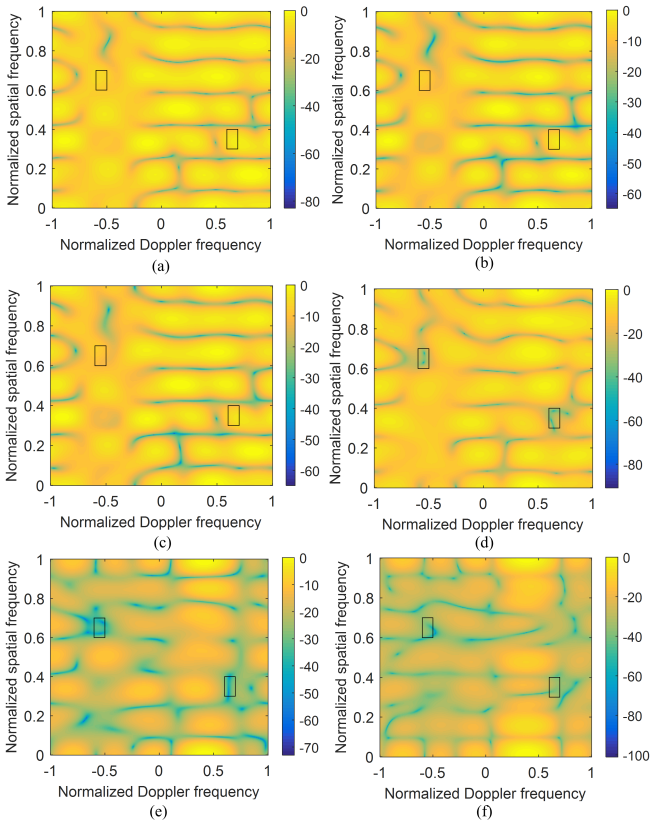

Fig. 2: spatial-frequency power spectra of designed waveforms, with (a) SDP-R $\xi_0 = 0.4$, (b) SDP-R $\xi_0 = 1$, (c) SDP-R $\xi_0 = 1.6$, (d) proposed $\xi_0 = 0.4$, (e) proposed $\xi_0 = 1$, (f) proposed $\xi_0 = 1.6$.

6. REFERENCES

[1] Z. Cheng, B. Liao, Z. He, Y. Li, and J. Li, "Spectrally compatible waveform design for MIMO radar in the presence of multiple targets," *IEEE Trans. Signal Process.*, vol. 66, no. 13, pp. 3543-3555, Jul. 2018.

[2] J. Qian, M. Lops, L. Zheng, X. Wang, and Z. He, "Joint system design for coexistence of MIMO radar and MIMO communication," *IEEE Trans. Signal Process.*, vol. 66, no. 13, pp. 3504–3519, 2018.

[3] F. Liu, L. Zhou, C. Masouros, A. Li, W. Luo, and A. Petropulu, "Toward dual-functional radar-communication systems: optimal waveform design," *IEEE Trans. Signal Process.*, vol. 66, no. 16, pp. 4264–4279, 2018.

[4] S. M. O'Rourke, P. Setlur, M. Rangaswamy, and A. Lee Swindlehurst, "Quadratic semidefinite programming for waveform-constrained joint filter-signal design in STAP," *IEEE Trans. Signal Process.*, vol. 68, pp. 1744-1759, Mar. 2020.

[5] B. Tang and J. Tang, "Joint design of transmit waveforms and receive filters for MIMO radar space time adaptive processing," *IEEE Trans. Signal Process.*, vol. 64, no. 18, pp. 4707-4722, May. 2016.

[6] S. Shi, Z. He, and Z. Wang, "Joint design of transmitting waveforms and receiving filter for MIMO-STAP airborne radar," *Circuits, Syst., Signal Process.*, vol. 39, pp. 1489-1508, Jul. 2019.

[7] B. Tang, J. Tuck, and P. Stoica, "Polyphase waveform design for MIMO radar space time adaptive processing," *IEEE Trans. Signal Process.*, vol. 68, pp. 2170-2181, Mar. 2020.

[8] J. Li, G. Liao, Y. Hang, Z. Zhang, and A. Nehorai, "Riemannian geometric optimization methods for joint design of transmit sequence and receive filter on MIMO radar," *IEEE Trans. Signal Process.*, vol. 68, pp. 5602-5616, 2020.

[9] G. Sun, Z. He, J. Tong, X. Yu, and S. Shi, "Mutual information-based waveform design for MIMO radar space-time adaptive processing," *IEEE Trans. Geosci. Remote Sens.*, vol. 59, no. 4, pp.2909–2921, Apr. 2021.

[10] Y. Wang, W. Li, Q. Sun, G. Huang, "Robust joint design of transmit waveform and receive filter for MIMO radar space-time adaptive processing with signal-dependent interferences," *IET Radar Sonar Navig.*, vol. 11 no. 8, pp. 1321–1332, 2017.

[11] Q. Zhou, Z. Li, J. Shi, and Y. Mao, "Robust cognitive transmit waveform and receive filter design for airborne MIMO radar in signal-dependent clutter environment," *Digital Signal Process.*, vol. 101, Jun. 2020, DOI: https://doi.org/10.1016/j.dsp.2020.102709.

[12] H. Wang, "Robust waveform design for MIMO-OFDM-based STAP in the presence of target uncertainty," *IET Radar, Sonar, Navig.*, vol. 12, no. 9, pp. 1021-1027, Jun. 2018.

[13] H. Wang, "Robust waveform optimization for MIMO-OFDM-based STAP in the presence of environment uncertainty," *Circuits, Syst., Signal Process.*, vol. 38, pp. 1301-1317, 2019.

[14] J. Li and P. Stoica, "MIMO radar with colocated antennas," *IEEE Signal Process. Mag.*, vol. 24, no. 5, pp. 106–114, Sep. 2007.

[15] A. Aubry, A. De Maio, M. Piezzo, and A. Farina, "Radar waveform design in a spectrally crowded environment via nonconvex quadratic optimization," *IEEE Trans. Aerosp. Electron. Syst.*, vol. 50, no. 2, pp. 1138–1152, Apr. 2014.

[16] A. Aubry, V. Carotenuto, and A. De Maio, "Forcing multiple spectral compatibility constraints in radar waveforms," *IEEE Signal Process. Lett.*, vol. 23, no. 4, pp. 483–487, Apr. 2016.

[17] O. Mehanna, K. Huang, B. Gopalakrishnan, A. Konar, and N. D. Sidiropoulos, "Feasible point pursuit and successive approximation of non-convex QCQPs," *IEEE Signal Process. Lett.*, vol. 22, no. 7, pp. 804–808, Jul. 2015.

[18] X. Yu, K. Alhujaili, G. Cui, and V. Monga, "MIMO radar waveform design in the presence of multiple targets and practical constraints," *IEEE Trans. Signal Process.*, vol. 68, pp. 1974-1989, Mar. 2020.

[19] S. Boyd and L. Vandenberghe, *Convex Optimization*. Cambridge, U.K.: Cambridge Univ. Press, 2004.

[20] M. Grant and S. Boyd, "Cvx package," Feb. 2012. [Online]. Available: http://www.cvxr.com/cvx.r.

[21] G. Cui, H. Li and M. Rangaswamy, "MIMO radar waveform design with constant modulus and similarity constraints," *IEEE Trans. Signal Process.*, vol. 62, no. 2, pp. 343-353, Jan. 2014.

[22] X. Yu, G. Cui, J. Yang, and L. Kong, 'MIMO Radar Transmit–Receive Design for Moving Target Detection in Signal-Dependent Clutter', *IEEE Trans. Veh. Technol.*, vol. 69, no. 1, pp. 522–536, Jan. 2020.